COLLISION AVOIDANCE FRAMEWORK FOR AUTONOMOUS VEHICLES UNDER CRASH IMMINENT SITUATIONS

by

Runjia Du

A Thesis

Submitted to the Faculty of Purdue University

In Partial Fulfillment of the Requirements for the degree of

Master of Science in Civil Engineering

Lyles School of Civil Engineering

West Lafayette, Indiana

December 2020

THE PURDUE UNIVERSITY GRADUATE SCHOOL
STATEMENT OF COMMITTEE APPROVAL

Dr. Samuel Labi, Chair
Lyles School of Civil Engineering

Dr. Jon D. Fricker
Lyles School of Civil Engineering

Dr. Hua Cai
School of Industrial Engineering

Approved by:
Dr. Dulcy Abraham

Dedicated to your custom dedication

ACKNOWLEDGMENTS

I acknowledge my thesis committee chair (Dr. Samuel Labi) and committee members (Dr. Jon D. Fricker and Dr. Hua Cai) for their immense support in various ways. I also acknowledge the Center for Connected and Automated Transportation (CCAT) for funding my graduate study. Finally, my dearest gratitude goes to my family for their patience and help throughout my studies. The thesis would not have been written without them and I truly cannot thank them enough for their understanding and unconditional support throughout my life.

TABLE OF CONTENTS

LIST OF FIGURES

LIST OF ABBREVIATIONS

abbreviation	definition
AV	Autonomous Vehicle
CAV	Connected Autonomous Vehicle
CHDV	Connected Human-driven Vehicle
FHDV	Following Human-driven Vehicle
FHDV-f	Following Human-driven Vehicle in the following position
FHDV-p	Following Human-driven Vehicle in the preceding position
HDV	Human-driven Vehicle
LHDV	Lane-changing Human-driven Vehicle
MPC	Model Predictive Control
NHTSA	National Highway Traffic Safety Administration
PHDV	Preceding Human-driven Vehicle
PHDV-f	Preceding Human-driven Vehicle in the following position
PHDV-p	Preceding Human-driven Vehicle in the preceding position
PID	Proportional-Integral-Derivative
QP	Quadratic Programming

ABSTRACT

Ninety-five percent of all roadway crashes are attributed fully or partially to human error, and a multitude of safety-related programs, policies, and initiatives have seen limited success in reducing roadway crashes and their accompanying fatalities, injuries, and property damage. For this reason, safety professionals have lauded the emergence of autonomous vehicles (AVs) as a promising palliative to the persistent problem of road crashes. Such optimism is reflected in recent literature that have argues from a conceptual standpoint, that road safety enhancement will be one of the prospective benefits of AV operations because automation removes humans from vehicle driving operations and therefore criminates or mitigates human error. It can be argued that the safety benefits of AVs will be manifest when AV market penetration reaches 100%. However, it seems clear from a practical standpoint that the transition from a system of exclusively human-driven vehicles (HDVs) to that of exclusively AVs will not only be necessary but also an arduous journey. This transition period will be characterized by heterogeneous traffic, where human-driven vehicles (HDVs) and AVs share the road space, and whence the prospective safety benefits of AVs may not be fully realized due to human error arising from the HDV operations in the mixed traffic space. These traffic conflicts, which may lead to collisions, could arise from any of several contexts of driving maneuvers, one of which is aggressive lane changes, the focus of this thesis. From the literature, it is clear that lane changing is inherently more collision-prone compared to most other maneuvers including car following, and therefore the consequences of errant human driving behavior such as inattention of misjudgment during lane changing, are more severe. To address this problem, this thesis developed a control framework to be used by AVs to help them avoid collision in a mixed traffic stream with human drivers who exhibit aggressive lane-changing behavior. The developed framework, which is based on a Model Predictive Control (MPC) approach, is designed to control the AV's movements safely by duly accommodating potential human error from the HDVs that could otherwise lead to any of two common collision patterns: rear-end and side-impact. Further, the thesis investigated how connectivity between the HDVs, and AVs could facilitate joint operational decision-making and sharing of real-time information, thereby further enhancing the safety of the entire traffic stream. Finally, the thesis presents the results of driving simulations carried out to test and validate the performance of the control framework under different traffic conditions.

1. INTRODUCTION

1.1 Background

1.1.1 Safety in traffic operations

Traffic-related fatalities and injuries continue to pose a global concern. A recent report on traffic safety reports that there were 1.25 million accidents in 2013 alone, and that in 30% of countries, fatalities from traffic related accidents is currently on the increase (Moosavi et. al., 2019). Traffic-related accidents are the second leading cause of death between the age of 5 and 29, and the third leading cause of death between the age of 30 and 44 (Anjuman, et. al., 2020). In 2018, more than 40,000 traffic-related fatalities occurred in the US (National Safety Council, 2018), and hundreds of thousands injured. With increasing travel demand, traffic fatalities and injuries may increase.

To combat the problem of traffic crashes, countries continue to pursue global and local initiatives. These initiatives address at least one of several strategic areas including road-use policy (regarding vehicle and driver roadworthiness) (Labi et al., 2017), roadway design (Chen et al., 2017; Tang et al., 2018; Chen et al., 2019), driver education, and in-vehicle design and features. For example, Vision Zero, a global effort, endeavors to eliminate traffic fatalities. However, studies have shown that 95% of crashes are related directly or indirectly to human error (NHTSA, 2016). Thus, while significant endeavors have been made to address roadway and other factors, such efforts directly address only 5% of all crashes.

With the rapid development of the vehicular automation and connectivity, reaching Vision Zero has become an achievable goal. Automation eliminates or drastically minimizes the human element in vehicle control, and therefore can directly address the 95% of accident sources (Rahman et. al., 2019; Noy et. al., 2018; Ye and Yamamoto, 2019; Chen et al., 2020). Interestingly, literature is replete with studies geared towards protecting the surrounding human drivers and pedestrians from errant AVs. On the other hand, there has been relatively little or no investigation into how an AV should maneuver in order to protect itself, and consequently the local traffic, from reckless human drivers. Therefore, this thesis focuses on developing an AV controller to facilitate the safety of vehicles in the neighborhood of the AV, to avoid imminent collision with errant HDVs.

1.1.2 Benefits of vehicle automation

Vehicle automation is expected to improve the transportation system safety, for the following reasons: (1) the reduced reaction time of vehicles due to the sensor fusion, which include cameras, radar, LiDAR, and Ultrasonic sensors (Figure 1.1); and (2) the elimination of the human element (mainly human error) in vehicle control.

Figure 1.1. Sensor fusion: camera, radar, LiDAR, Ultrasonic sensor

There is a significant amount of literature on the effectiveness of sensor-based visual target tracking of AVs (Jia et al., 2008; Lange and Detlefsen, 1991; Dickmann et. al., 2014). Vehicle automation can be expected to enhance the safety of the transportation system, providing benefits not only to AV users but also to the HDV users. There are a number of studies that recognize that failures in complex systems are often due to human errors (Christoffersen, and Woods, 2002). Automation, considered as a cognitive prosthesis, replaces human function to a large degree, devoid of common causes of human error (Sheridan and Parasuraman, 2005). Therefore, modification of a complex system by reducing human input has been understood as an appropriate way to enhance the system (Lee and Seppelt, 2006). In the context of transportation engineering, there exists great opportunity to enhance the safety of the roadway users by incorporating automation (Chen et al., 2019; 2020). However, despite the frequent discussions about the safety benefits of AVs, few studies have investigated how AVs will provide such safety benefits.

1.1.3 Benefits of V2V connectivity

A complementary, yet distinct technology that can further enhance the safety benefits of vehicular automation is V2V (vehicle to vehicle) connectivity. (Dong et al., 2020a, 2020b, 2020c; Li et al.,

2020a, 2020b) The V2V technology communicates information on the speed and position of surrounding vehicles through a wireless exchange information. In situations involving hazardous roadway conditions, drivers of connected human-driven vehicles (CHDVs) can receive warning notifications and alerts. V2V connectivity has key advantages over other emerging on-board technologies now appearing in high-end vehicles including radar, lidar, cameras and other sensors (USDOT, 2011).

First, with its larger range compared on-board equipment, V2V connectivity allows the driver to receive information much faster, thereby providing greater reaction time during emergencies. Secondly, V2V connectivity, unlike the on-board sensors, does not rely on any lines of "sight," and therefore is not prone to occlusion or inclement weather. In other words, a connected vehicle still receives the needed information even when it is out of sight from another vehicle or entity. Furthermore, connectivity technology is less expensive compared to sensor technologies; therefore, making it more affordable and practical for installation on AVs or HDVs. In past research (Talebpour & Mahmassani, 2014; 2016), assumptions of connectivity have been made in terms of the human reaction time but the transportation system safety impacts of connectivity, particularly of CHDVs were not stated clearly.

This thesis seeks to address the opposite perspective: the AV must avoid collision imminent situations posed by reckless HDV maneuvers. Existing studies on CAV controllers do not recognize (and therefore, fail to take advantage) of the presence of connected HDVs in the vicinity of the CAV. In reality, a CAV that is connected to its neighboring HDVs can serve as a centralized, local decision maker that, with the cooperation of the CHDVs, can control the trajectories of the neighboring vehicles in a holistic bid to maximize overall safety (by effectively responding to collision-imminent situations).

1.2 Problem statement

As discussed earlier in this chapter, traffic crashes can be significantly reduced by "taking the human from the steering wheel.", which can be most effective when the market penetration of AVs is 100%. However, in the HDV-AV transition phase where there will exist mixed traffic flow (both autonomous vehicle and human-driven vehicles in the traffic stream), human error will persist and therefore, the AV safety benefits will be limited. Nevertheless, several options exist to reduce or mitigate the errors that will be made by human-driven vehicles. One such option is to use vehicular

connectivity (V2V) to take over under emergency situations. Thus, this thesis presents a vehicle controller based on V2V that minimizes AV-HDV collision under imminent situations. Common types of motor vehicle accidents are as follows: vehicle rollover, single-car accidents, rear-end collisions, and side-impact collisions (National Safety Council, 2018; Xu et al., 2019). Therefore, this research considers the following collision scenarios: (1) side-impact collision and (2) read-end collision under a lane-change situation due to HDV driver error.

1.3 Research gaps and study objectives

Most existing studies focus primarily on how the AV can operate without compromising the safety of the Neighboring HDVs (Kalra and Paddock, 2016; Koopman and Wagner, 2017; Kim et al., 2019; Ko et al., 2015; Chen et. al., 2013; Naranjo et al., 2008). This thesis seeks to address the opposite perspective: the AV must avoid collision imminent situations posed by reckless HDV maneuvers. Existing studies on CAV controllers do not recognize (and therefore, fail to take advantage) of the presence of connected HDVs in the vicinity of the CAV. In reality, the CAV that is connected its neighboring HDVs can serve as a centralized cooperative decision maker (Dong et al., 2020a, 2020b, 2020c; Ha et al., 2020a, 2020b; Du et al., 2020) that, control the trajectories of the neighboring vehicles in a holistic bid to maximize overall safety (by effectively responding to collision-imminent situations).

The thesis focuses on incorporating the automation with the connectivity to enhance safety of a neighborhood of AVs and HDVs under emergency conditions. Also, the thesis attempts to justify the safety benefits of connectivity to all road users: for non-autonomous human-driven vehicles, the thesis intends to show how connectivity capabilities can help compensate for their lack of automation

2. LITERATURE REVIEW

2.1 Collision avoidance

With the increasing travel demand, traffic fatalities and injuries may increase. Collision avoidance needs to be focused particularly in the transition era where the traffic stream will be mixed (AVs and HDVs). However, as mentioned in the background section in Chapter 1 of this thesis, most previous research efforts were geared towards protecting the surrounding human drivers and pedestrians from errant AVs. Obviously, human error will exist in the mixed traffic flow as HDVs will be using the roads. Therefore, there is a need to investigate into how an AV should maneuver to protect itself. Also, it is need to investigate how the local traffic in the neighborhood of the AV can be protected from reckless HDVs through specific maneuvers of the AV. Most existing studies focus primarily on how the AV can operate without compromising the safety of the neighboring HDVs (Kalra and Paddock, 2016; Koopman and Wagner, 2017; Kim et al., 2019; Ko et al., 2015; Chen et. al., 2013; Naranjo et al., 2008).

2.2 Control methods

There are several simple but efficient controllers such as proportional–integral–derivative (PID) controllers, which is by far the dominant control structure in industrial practice (Arzén, 1999). However, the AV control problem in this thesis may not be amenable for PID use. Because the interaction between the LHDV and AV will affect the control input of the controller, we consider a motion prediction of the LHDV through the lane change process to give the control system more information as well as additional constraints. For each time step, the LHDV will generate different information to be captured by the controller in terms of the motion (position and velocity of LHDV). Thus, a critical consideration for the control framework in this thesis, is to have real-time control ability and the ability to handle multiple constraints.

MPC (model predictive control) also known as receding horizon control or moving horizon control, is widely accepted as the controller of choice for multivariable systems that have inequality constraints on system states, inputs and outputs (Bletis & Kothare, 2005). MPC is commonly used in dealing with real-time control problem with multiple constraints (Richter, 2009;

Richter, 2011; Zeilinger, 2011). MPC is based on iterative, finite-horizon optimization of a plant model. If the current control interval is assumed as k, then at time k, the current plant state is sampled, and a cost minimizing control strategy is computed for a horizon T in the future. The method emanates from the current state and identifies a cost-minimizing control strategy over a time horizon T', which is called control horizon. Only the first step of the control strategy is implemented, and then the plant state is sampled again, and the calculations are repeated starting from the new current state, ultimately yielding the final control strategy. MPC is capable of handling multiple inputs and outputs. It is a multivariable control algorithm that uses: 1. Internal dynamic model of the process. 2. Cost function over the prediction horizon. 3. Optimization problem that minimizing the cost function based on the control inputs. The basic MPC cost function for the optimization can be written as:

$$J = \sum_{k=1}^{T} \omega_k \|y_k - r_k\|^2 + \sum_{k=1}^{T'} \varphi_k \|u_k - u_{k-1}\|^2$$

Where: y_k represents for the states of the system, and r_k represents for the reference of the system. u_k here is the control input. φ_k and ω_k are the weights of the cost function.

2.3 Application of model predictive control in collision avoidance

Model predictive control (MPC) is an effective approach for solving problems that arise from motion planning. The MPC approach entails that the motion planning problem is formulated as an optimization problem, often as a constrained, convex problem solved in a recursive manner by considering the updating of the environment states during the planning process. In literature, MPC is frequently used for motion planning problems (Babu et al., 2019; Wang et al., 2019; Shen et al., 2017; Werling et al., 2012; Ji et al., 2016). Specifically, these studies used MPC to solve the problem of vehicle path generation to mitigate collision. However, they focused on human error from inside the vehicle. Human error from outside the AV in the mixed traffic flow, was not considered. Further, despite the popularity of MPC for vehicular motion planning, it is essential to understand and address the shortcomings that arise in the use of this approach. Specifically, MPC does not necessarily result in closed loop stable systems. It is common to include in the control architecture, a final state constraint or a final state penalty that helps achieve stability of the output. However, when the controller structures are too complicated, the constraint set consists of many

inequalities, and subsequently it is difficult to guarantee stability of the outcome using the final state constraint.

For this reason, researchers have explored various ways of testing and validating the stability of MPC controllers. Di et al. (2009) used the controller matching technique and provided two methods for selecting the MPC weight matrices so that the resulting MPC controller behaves as the given linear controller. This ensures that the inverse problem of controller matching is solved, and that the solution is globally asymptotically stable (Di Cairano, 2009).

Another way is to identify the sufficient condition for stability of the closed loop system. Specifically, using the Lyapunov function as the cost function, an optimization problem can be formulated as: $min(V_k^* - V_{k+1}^*)$, where V_k^* refer to the objective function at time k and V_{k+1}^* refer to the objective function at time k+1 respectively. For the MPC with different prediction horizon N, if there exist negative $min(V_k^* - V_{k+1}^*)$, then the Lyapunov function V_k is improper for the system to be stable. However, if all the difference values are positive, then the V_k is a proper Lyapunov function under the prediction horizon N (Simon & Löfberg, 2016).

3. METHOD

3.1 Problem formulation

3.1.1 Problem settings

Side-impact collisions, which affect the side of one or multiple vehicles, includes accidents where the vehicle glances off the side or near-side of another vehicle; the lateral impact is the primary impact rather than the front or rear. Many side-impact crashes happen when drivers on a multi-lane highway change lane without observing the vehicle in their blind spot and collides in the target lane. Rear-end collisions occur when a vehicle crashes into the rear of vehicle in front (Herrman, 2016). However, the most common exception to the general presumption about rear-end collision accidents involves another vehicle on the freeway that suddenly changes lanes and enters the target lane. Rear-ending commonly occurs when there is traffic or an accident up ahead in the driver's original lane. Upon such realization of a traffic problem in their lane downstream, the drivers typically choose to perform a sudden lane change instead of slowing down or fully stop. However, on the freeway, traffic on the target lane typically travels much faster compared to traffic on the driver's original lane, which will very likely lead to a rear-end collision. Examples of the two crash patterns are shown in Figure 3.1.

This research focuses on the safety effects given by combining the automation and connectivity in mixed traffic flow. The vehicles included in this research are as follows (Figure 3.1): connected autonomous vehicle (CAV, colored red); lane changing human-driven vehicle (LHDV, colored gray), which do not have connectivity; and connected human-driven vehicles (CHDVs) in the following and preceding positions (FHDV colored blue, and PHDV colored yellow, respectively).

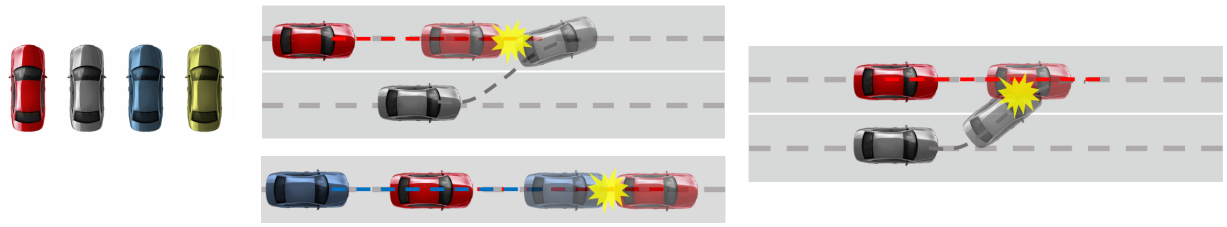

LEGEND
CAV (red), HDV (grey), CHDV (following blue; preceding yellow)

Rear-end collision

Side-impact collision

(b). crash patterns example

Figure 3.1. Two crash patterns (rear-end, side-impact)

Crash patterns

Side-impact collision: The side-impact collision also known as broadside or T-bone collisions, where the side of one or multiple vehicles is impacted. Side-impact collisions also include accidents in which a vehicle glances off the side or near-side of another vehicle, where the lateral impact is the primary impact rather than the front or rear. For instance, many side-impact crashes happen when drivers on a multi-lane highway changes lane without observing the vehicle in his/her blind spot, and swerves into the target lane.

Rear-end collision: Normally, rear-end collision is regarded as a traffic accident where a vehicle crashes into the vehicle in front of it. However, the most common exception to the general presumption about rear end collision accidents involves another vehicle on the freeway suddenly changes lanes and enters to the target lane. This commonly happens when there is traffic or an accident up ahead in the driver's original lane. Drivers usually choose to do the sudden lane change instead of slowing down or fully stop. However, on the freeway, traffic on the target lane usually travels much faster compared to traffic on the driver's original lane, which will very likely lead to rear-end collision.

Avoidance maneuvers

The two CAV crash avoidance maneuvers (Figure 3.2) are considered based on the combination of the collision types and vehicle types. The first scenario is the deceleration maneuver of the CAV

to avoid the potential rear-end collision by the lane changing human-driven vehicle (LHDV) as shown in Figure 3.2(a). In the second scenario, the longitudinal positions of the LHDV and CAV are nearly the same. Once the LHDV lane-changing process begins, it's hard for CAV to avoid the collision even by using the maximum deceleration. Thus, the autonomous vehicle only has the choice of lane change to the opposite lane to avoid the possible side-impact collision as shown in Figure 3.2(b).

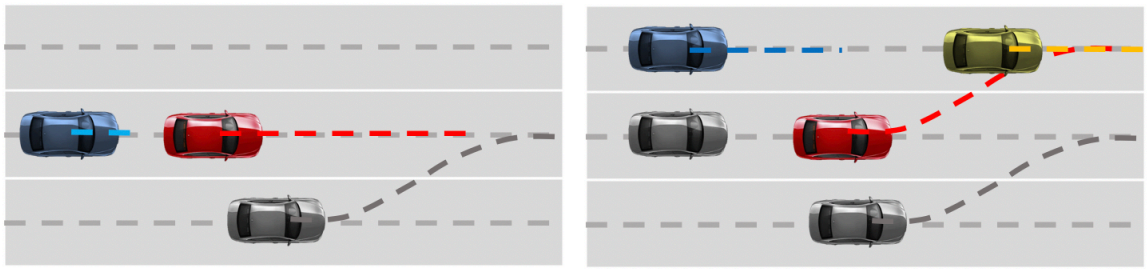

(a). deceleration maneuver (b). lane-changing maneuver

Figure 3.2. Different CAV crash-avoidance maneuvers

3.1.2 Assumptions

The following assumptions have been made in this thesis:

(1) Vehicles are all light passenger vehicles, and the vehicle length is 4 meters, the diameter of buffer circles is 6 meters, the lane width is 3.7 meters.
(2) Initial speeds of the vehicles on the road are in a proper range, considering the reality.
(3) The lane changing trajectory of the LHDV is assumed to be cubic polynomial and is predicted accurately. This is based on a previous research in the literature (Yang et al., 2018).
(4) The latitudinal position of the CAV in the deceleration maneuver and the latitudinal positions of CHDVs on the target lane are constants, indicating CAV and CHDVs on the target lane do not perform lane change.
(5) The LHDV acceleration is assumed to be highly aggressive with little regard of its surroundings. The exact numerical specifications are explained in the simulation section.
(6) The vehicles' velocities are uniformly distributed.

In order to make more obvious the safety benefits, each vehicle is represented by a circle buffer area. Figure 3.3 illustrate how the buffer area works in this research. In the lane-changing process, the buffer circles need to avoid tangent or intersect situations to avoid the crashes.

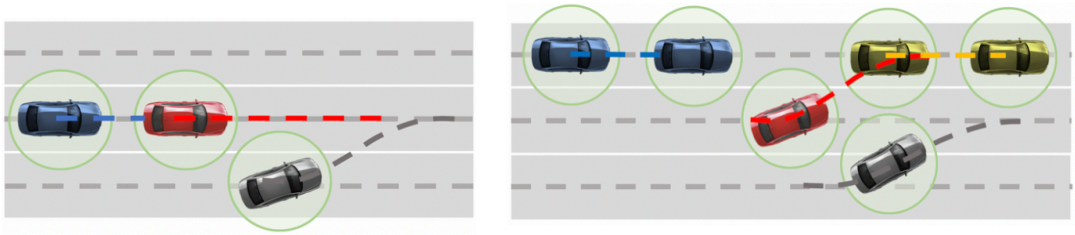

Figure 3.3. Vehicle buffer area

3.2 Proposed approach

This section presents the overall control framework of the controller. The detailed motion prediction model which considers the interactions between the LHDV and the CAV is introduced as well. In addition, the motion models of the controlled vehicles are formulated in this section in terms of deceleration and acceleration. The objective of the mathematical model in this research is to determine the optimal crash avoidance maneuvers, which includes the optimal deceleration decisions and corresponding optimal deceleration/acceleration decisions in the lane changing. The optimal maneuvers consider the LHDV-CAV interactions and CAV-surrounding CHDVs interactions. In order to determine the optimal control maneuvers, the problem is formulated as a bi-level optimization problem. The methodology consists of the following components: 1). control framework, 2). LHDV motion prediction, 3). controlled vehicles motion model, 4). the optimization problems to solve for deceleration and lane change maneuvers, and 5). the stability of the controller.

3.2.1 Control Framework

The proposed control framework deals with multiple vehicles in a crash-imminent situation. Thus, the controller needs to perform actions and deal with multiple constraints in real-time. As discussed previously, an MPC controller is suitable for this purpose. The motion of the LHDV is regarded as important reference for the CAV. The interactions between the LHDV and the controlled CAV, the motion of the surrounding CHDVs are crucial for the MPC controller. Figure 3.4 shows the general structure of the proposed control framework. In this research, there are two CAV reaction maneuvers considered: deceleration and lane change. The CAV controller considers the maneuvers in a hierarchical structure, first considering the deceleration maneuver, as it is less disruptive. Should deceleration be insufficient or inadequate for a given crash-imminent situation,

it will engage in the lane-change maneuver. The MPC is formulated as an optimization problem and will be solved each time step to generate the optimized deceleration for CAV and FHDV or the optimized acceleration/deceleration for PHDV and FHDV. The detailed structure of the MPC based controller is described in Figure 3.4.

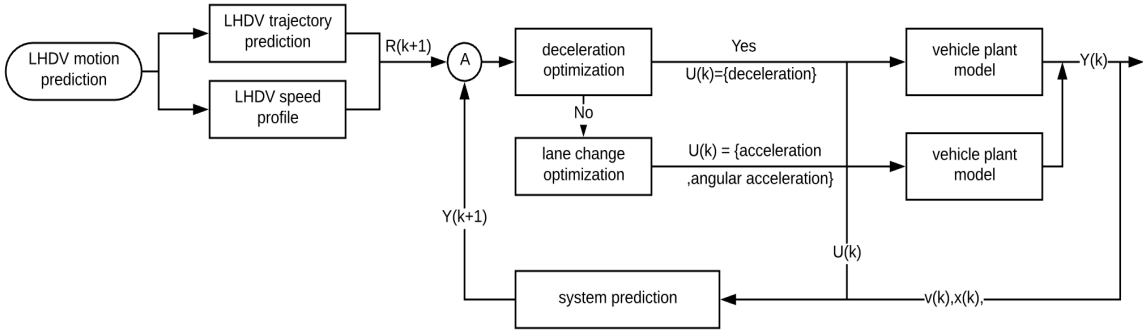

Figure 3.4. Control framework

3.2.2 LHDV motion prediction model

Motion prediction includes two parts: trajectory prediction and speed profile generation. The LHDV is uncontrollable, and the motions are unstable. The trajectory of the aggressive LHDV is incorporated into the CAV controller, and the predicted aggressive trajectory is assumed to be cubic polynomial (Yang et al., 2018), which has second-order smoothness. The speed profile is then calculated based on the aggressive behavior and the rollover limit of the vehicle.

Trajectory predicting model

The position and velocity of the LHDV are continuous because the cubic polynomial curve ($y(x) = ax + bx^2 + cx^3$) is second-order differentiable. The LHDV positions are represented by (x_t, y_t), where x_t and y_t denote the longitudinal and latitudinal positions of time step t. θ represents the course angle of the LHDV, which is the angle between the moving direction U (in the Figure 3.5) and the $x - axis$. The ending position of the lane change trajectory is calculated by implementing rollover-free conditions, which are represented by (x_t^e, y_t^e), the final position's course angle ($\theta_e = 0$;$y_t'(x_t^e)$=0). Rollover collision is a single-car accident that can happen when the lane-changing vehicle is behaving aggressively, and the velocity is too large. However, in this

research, the collision we focused on is multi-car accidents. Thus, the rollover-free condition avoids the single-car accident but maintains the aggressiveness of the lane-changing vehicle.

The rollover-free boundary can be represented by the y_t^e and the rollover side acceleration boundary, which is a_s^r. Thus, the rollover boundary for the final longitudinal position of the LHDV is:

$$x_t^r = \sqrt{6}\frac{y_t^e u_t^i}{\sqrt{y_t^e a_s^r}} \tag{1}$$

the value of a_s^r is set as 0.71g m/s^2(Gluckman, 2011), u_t^i is the initial condition (i) velocity on the moving direction of time step t.

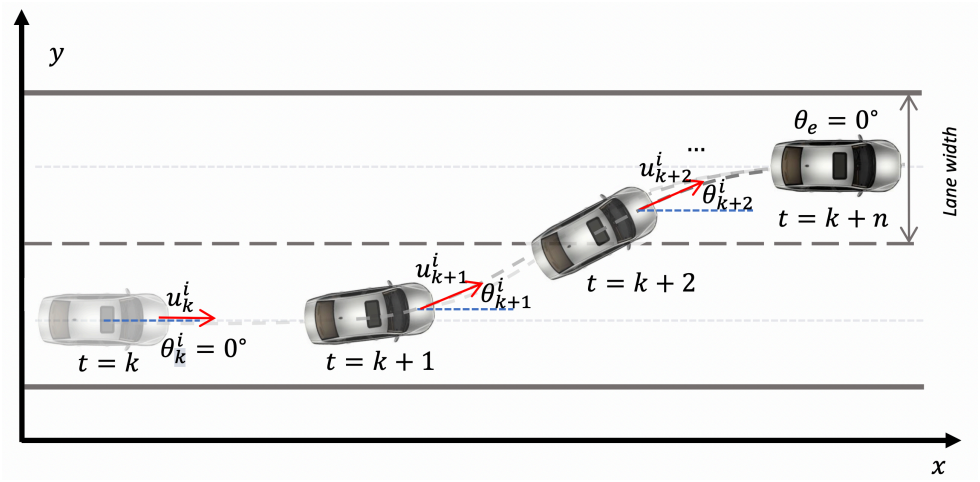

Figure 3.5. Aggressive rollover-free trajectory and representation

To avoid a rollover collision, the final position x_t^e equals to the rollover boundary x_t^r considering the most aggressive case. Figure 3.5 presents the lane changing trajectory. The moving coordinate system is used here to model a dynamic lane changing maneuver. The initial course angle of the trajectory θ_t^i of time step t must satisfy $y_t'(x_t) = tan\theta_t^i$ From the ending position of the course angle, we know that $y_t(x_t^e) = 0$. Hence, the optimal trajectory is:

$$y_t(x_t) = tan\theta_t^i x_t + \frac{3y_t^t - 2x_t^e tan\theta_t^i}{(x_t^e)^2}x_t^2 + \frac{x_t^e tan\theta_t^i - 2y_t^e}{(x_t^e)^3}x_t^3 \tag{2}$$

Consider an initial LHDV velocity of 50 miles per hour. Then the longitudinal final position $x_t^r = \sqrt{6}\frac{y_t^e u_t^i}{\sqrt{y_t^e a_s^r}} \approx 86$ meters. For example, in Figure 3.6: the trajectory in each time step can be generated by the new desired ending position, new angle, latitudinal distance. The lines in the figure represent the predicted trajectory of different time steps. When the location and velocity are updated in a new time step, the predicted trajectory changes accordingly.

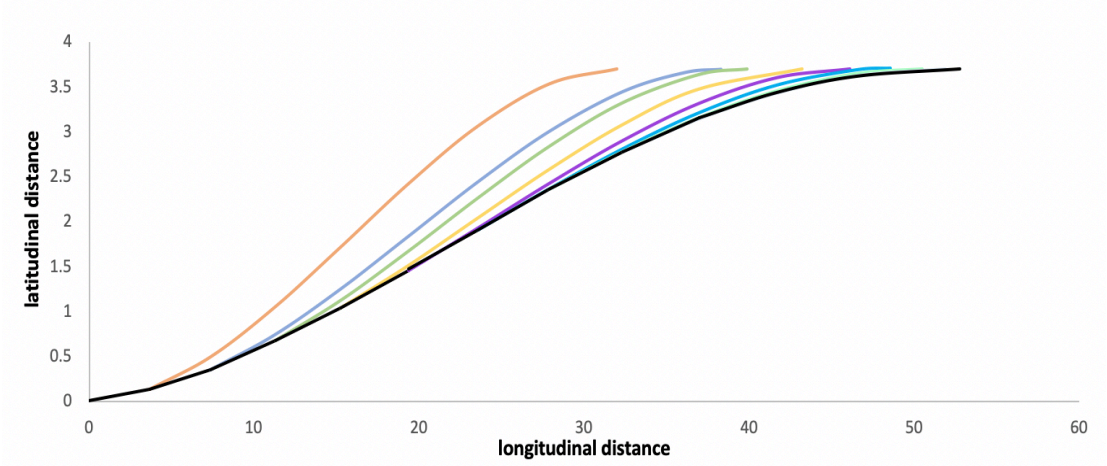

Figure 3.6. Predicted trajectory of LHDV in each time steep

Speed profile predicting model

The LHDV driver is assumed to be highly aggressive in accelerating into the target lane. The most aggressive longitudinal distance can be calculated based on the rollover limit, with initial velocity u_t^i at time step t. Then the aggressive acceleration can be calculated based on the rollover limit as well as the length of each time step: τ.

$$a = \frac{2\left(\frac{6y_t^e u_t^i}{\sqrt{6y_t^e a_s^r}} - u_t^i \tau\right)}{\tau^2} \qquad \textbf{(3)}$$

If we assume the highest longitudinal acceleration rate is a_{max}, then the proper aggressive longitudinal acceleration can be represented as $min\{a, a_{max}\}$. Based on the acceleration, the aggressive velocity of the time step t is therefore $u_n^i + \min\{a, a_{max}\}\tau$. The important information for each time step that will be used in the control framework is the longitudinal location, latitudinal

location and moving direction angle of LHDV at each time step. First step, the trajectory curve is calculated through the v_t^i (initial longitudinal velocity) and v_t^e (ending longitudinal velocity) of LHDV: $L = \frac{(v_t^i + v_t^e)\tau}{2}$. The longitudinal position of the LHDV at each time step can be calculated by solving Equation (4):

$$\frac{(v_t^i + v_t^e)\tau}{2} = F(x_t^e) - F(0) \quad \textit{(4)}$$

$F(x_t)$ is the antiderivative of the $f(x_t)$

$$f(x_t) = \sqrt{1 + \left(tan\theta_t^i + \frac{6y_t^e - 4x_t^e tan\theta_t^i}{{x_t^e}^2} x_t^2 + \frac{3x_n^f tan\theta_i - 6y_n^f}{{x_n^f}^3} x_n^3 \right)^2} \quad \textit{(5)}$$

Thus, the latitudinal position can also be determined by the trajectory $y_n(x_n)$. The moving direction at the end each time step can be calculated as follows:

$$tan\theta_t^e = tan\theta_t^i + \frac{3y_t^e - 2x_t^e tan\theta_t^i}{{x_t^e}^2} x_t + \frac{x_t^e tan\theta_t^i - 2y_t^e}{{x_t^e}^3} x_t^2 \quad \textit{(6)}$$

3.2.3 Controlled vehicles motion model

The controlled vehicles in this thesis research are the autonomous vehicles and the surrounding HDVs that are connected, i.e., the FHDV and PHDV. For the FHDV, the motion model is based on deceleration and PHDV, the motion model is based on acceleration remains. However, the constraints in the optimization problem for different controlled vehicles may change accordingly. For the deceleration scenario, the motion model of the CAV and FHDV is given by the deceleration model (Equations 7-1 to 7-6).

Deceleration

$$x(k+1) = x(k) + v(k)\Delta t + \frac{1}{2} d(k) \Delta t^2 \quad \textit{(7-1)}$$

$$y(k+1) = y(k) = constant \quad \textit{(7-2)}$$

$$v(k+1) = v(k) + d(k)\Delta t \quad \textit{(7-3)}$$

$$X(k+1) = AX(k) + BU(k) \quad \textit{(7-4)}$$

$$Y(k+1) = CX(k+1) \quad \textit{(7-5)}$$

$$for: X(k) = \begin{bmatrix} x(k) \\ v(k) \end{bmatrix}, A = \begin{bmatrix} 1 & \Delta t \\ 0 & 1 \end{bmatrix}, B = \begin{bmatrix} 1/2\Delta t \\ \Delta t \end{bmatrix}, U(k) = d(k) \quad \textit{(7-6)}$$

Where: $x(k), v(k)$ and $d(k)$ are the longitudinal position, velocity and the deceleration, respectively, of the controlled vehicles. The controlled variables are $d(k)$. In the lane change scenario, the motion model of PHDV based on the acceleration, where $x(k), v(k)$ represent the location and the velocity. The controlled variable is the acceleration $a(k)$, given by the acceleration model (Equations 8-1 to 8-6).

Acceleration

$$x(k+1) = x(k) + v(k)\Delta t + \frac{1}{2}a(k)\Delta t^2 \quad \textit{(8-1)}$$

$$y(k+1) = y(k) = constant \quad \textit{(8-2)}$$

$$v(k+1) = v(k) + a(k)\Delta t \quad \textit{(8-3)}$$

$$X(k+1) = AX(k) + BU(k) \quad \textit{(8-4)}$$

$$Y(k+1) = CX(k+1) \quad \textit{(8-5)}$$

$$for: X(k) = \begin{bmatrix} x(k) \\ v(k) \end{bmatrix}, A = \begin{bmatrix} 1 & \Delta t \\ 0 & 1 \end{bmatrix}, B = \begin{bmatrix} 1/2\Delta t \\ \Delta t \end{bmatrix}, U(k) = d(k) \quad \textit{(8-6)}$$

3.2.4 Deceleration Maneuver MPC Controller Design and Optimization

Vehicles interaction

When their relative speeds and distances are large enough, vehicles can be represented as particles. However, under a collision-imminent situation, appropriate representation of vehicle dimensions is critical. In this thesis, each vehicle is represented as enclosed circles with a diameter length equal to 1.5 times the vehicle length. The collision point of the CAV and LHDV is another critical factor

for the controller, as this information is directly used to decide a proper prediction horizon size N_p. In addition, the reference for the MPC controller depends on the longitudinal distance of LHDV and the velocity of each time step.

As shown in Figure 3.7, the critical point can be calculated by the tangent of the two circle centers representing the LHDV and CAV for each time step: $(x_{LHDV} - x_{AV})^2 + (y_{AV} - y_{LHDV})^2 = 4r^2$. The longitudinal distance of the CAV is smaller than the longitudinal distance of the LHDV by a constant, l_1. During the lane changing process, the velocity of the CAV needs to be less than or equal to the velocity of the LHDV, but with a soft constraint, the velocity can be greater than the velocity of the LHDV through the process. For the last time step, the velocity of the CAV is required to be strictly lesser than or equal to the velocity of the LHDV. From the speed profile, the speed at the end of each time step can be computed.

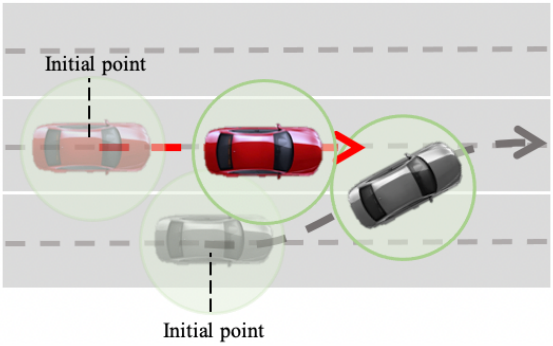

Figure 3.7. LHDV-CAV interaction

While the CAV's crash avoidance maneuvers are affected by the behavior of the LHDV. In the deceleration scenario, the FHDV affects the deceleration rate of the CAV, with the maximum deceleration threshold being relaxed with connectivity. As shown in Figure 3.8, the challenge arises as the CAV must satisfy the maximum deceleration threshold of both itself and the FHDV to avoid a secondary collision that caused by the lane-changing collision, entailing a feasible deceleration range for the CAV to follow: $\max\{f(d_{FHDV}^{max}), d_{AV}^{max}\}$.

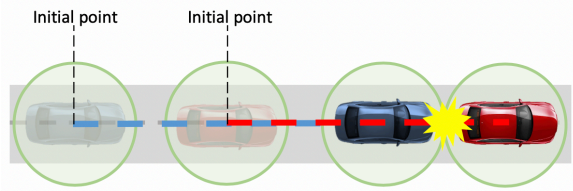

Figure 3.8. CAV-FHDV interaction

To further improve the system safety, the distance between the FHDV and the CAV must maintain a value greater than or equal to l_2, which directly affects the headway. Thus, the reference value of the FHDV is the CAV's longitudinal distance x_{AV} and the velocity v_{AV} at each time step. The maximum deceleration rate of the FHDV is d_{FHDV}^{max}, determined by both the comfortability and the security. The deceleration of the CAV given the FHDV is as follows:

$$f(d_{FHDV}^{max}) = \frac{2l_2 - 2(\Delta x + \Delta v\tau)}{\tau^2} + d_{FHDV}^{max} \quad \textbf{(9)}$$

Where:

$\Delta x = x_{AV}^i - x_{FHDV}^i$, which is the initial distance between the CAV and FHDV. $\Delta v = v_{FHDV}^i - v_{AV}^i$.

Deceleration maneuver controller design

Compared to other controllers such as the PID controller (Rivera et al., 1986), the MPC controller (Camacho & Alba, 2013) can predict the states of the system in multiple sampling times, and therefore resulting a more accurate control decision. N_p represents the prediction horizon, which is the number of future control intervals that the MPC evaluates. N_c represents the control horizon, which is the number of control actions to be optimized in the control interval. Based on the MPC control strategy, the initial value is implemented, and the calculations will be repeated at each time step. The predicted output for control interval i can be represented by the system of Equations 10-1 to 10-6:

$$x(k+1) = Ax(k) + Bu(k) \quad \textbf{(10-1)}$$

$$x(k+2) = A^2x(k) + ABu(k) + Bu(k+1) \quad \textbf{(10-2)}$$

$$x(k+3) = A^3x(k) + A^2Bu(k) + ABu(k+1) + Bu(k+2) \quad \textbf{(10-3)}$$

…

$$x(k+N_c) = A^{N_c}x(k) + A^{N_c-1}Bu(k) + \cdots + Bu(t+N_c-1) \quad \textbf{(10-4)}$$

$$x\big(k+N_p\big) = A^{N_p}x(k) + A^{N_p-1}Bu(k) + \cdots + ABu(k+N_c-1) + Bu(t+N_c-1) \quad \textbf{(10-5)}$$

$$for: X(k) = \begin{bmatrix} x(k) \\ v(k) \end{bmatrix}, A = \begin{bmatrix} 1 & \Delta t \\ 0 & 1 \end{bmatrix}, B = \begin{bmatrix} 1/2\Delta t \\ \Delta t \end{bmatrix}, U(k) = d(k) \quad \textbf{(10-6)}$$

Thus, the output sequence and input sequence are defined in matrix form as follows:

$$X(k+1)=\begin{bmatrix} x(k+1) \\ x(k+2) \\ x(k+3) \\ \vdots \\ x(k+N_p) \end{bmatrix}_{N_p\times 1} \qquad U(k)=\begin{bmatrix} u(k) \\ u(k+1) \\ \vdots \\ u(k+N_c-1) \end{bmatrix}_{N_c\times 1} \tag{11}$$

The system prediction can be rewritten as $X(k+1)=M_x x(k)+M_u U(k)$:

$$M_x=\begin{bmatrix} A \\ A^2 \\ \vdots \\ A^{N_p} \end{bmatrix}_{N_p\times 2} \quad and\ M_u=\begin{bmatrix} B & 0 & \dots & \dots & 0 \\ AB & B & 0 & \vdots & 0 \\ \vdots & \vdots & \ddots & \vdots & \vdots \\ A^{N_c-1}B & A^{N_c-2}B & \dots & \ddots & B \\ A^{N_p-1}B & A^{N_p-2}B & \dots & \dots & (A+1)B \end{bmatrix}_{2N_p\times N_c} \tag{12}$$

For the deceleration maneuver, the primary goal is for the CAV to avoid collision by reducing its velocity. Thus, the controlled vehicles considered in this optimization problem are the CAV and the FHDV. The controller must satisfy both distance and velocity requirements in order to successfully avoid collision. Since the FHDV's control decision will be affected by the CAV's action, the problem can be formulated as a bi-level optimization, which formulated as:

$$\begin{aligned} &\min_{u_{AV}\delta_{AV},u_{FHDV},\delta_{FHDV}} F(u_{AV},\delta_{AV},u_{FHDV},\delta_{FHDV}) \\ &subject.to. \\ &u_{AV},\delta_{AV}\in \underset{u_{AV},\delta_{AV}}{\operatorname{argmin}}\{f(u_{AV},\delta_{AV},u_{FHDV},\delta_{FHDV}): g_j(u_{AV},\delta_{AV},u_{FHDV},\delta_{FHDV})\le 0, j=1,\dots,J\} \\ &G_i(u_{AV},\delta_{AV},u_{FHDV},\delta_{FHDV})\le 0, i=1,\dots,I \end{aligned} \tag{13}$$

For the upper level, the cost function includes the control input variables of both the CAV and the FHDV. At the lower level, however, the control input of CAV needs to fulfill the safety requirements of the LHDV. Therefore, the detailed objective function and constraints can be formulated as follows:

Upper level: CAV+FHDV

$$\min_{\substack{u_{AV}\\ \delta_{AV}\\ u_{FHDV}\\ \delta_{FHDV}}} \sum_{n=1}^{N_p} \|x_{FHDV}(k+n) - x_{AV}(k+n)\|_Q^2 + \sum_{n=1}^{N_c} \|u_{AV}(k+n-1)\|_R^2 + \|u_{FHDV}(k+n-1)\|_R^2 + \|\delta_{AV}(k+n-1)\|_P^2 + \|\delta_{FHDV}(k+n-1)\|_P^2 \quad \textbf{(14)}$$

s.t. $.(n = 1, \dots, N_p)$

$$u_{AV}, \delta_{AV} \in \underset{u_{AV},\delta_{AV}}{\operatorname{argmin}}\{f(u_{AV}, \delta_{AV}, u_{FHDV}, \delta_{FHDV}): g_j(u_{AV}, \delta_{AV}, u_{FHDV}, \delta_{FHDV}) \le 0, j = 1, \dots, J\} \quad \textbf{(14-1)}$$

$$x_{FHDV}(k+1) = Ax_{FHDV}(k) + Bu_{FHDV}(k) \quad \textbf{(14-2)}$$

$$x_{FHDV}(k+n) - x_{AV}(k+n) + \begin{bmatrix} l_2 \\ -\delta_{FHDV}(n) \end{bmatrix} \le 0 \; for \; n = 1, \dots, N_c \quad \textbf{(14-3)}$$

$$x_{FHDV}(k+n) - x_{AV}(k+n) + \begin{bmatrix} l_2 \\ 0 \end{bmatrix} \le 0 \; for \; n = N_p \quad \textbf{(14-4)}$$

$$d_{FHDV}^{max} \le u_{FHDV}(k+n-1) \le 0 \quad \textbf{(14-5)}$$

$$\delta_{FHDV}(k+n) \ge 0 \; n = 1, \dots, N_p \quad \textbf{(14-6)}$$

Note that the upper-level constraints do not bind the lower-level decision variables, which are u_{AV}, δ_{AV}. Thus, on the upper level, the constraints apply to u_{FHDV}, δ_{FHDV}. Taking the safety requirements into consideration, the FHDV and the CAV need to keep a longitudinal distance difference no less than l_2 throughout the prediction horizon N_p, and the speed of the FHDV of each time step needs to be no larger than that of the CAV by a small positive value, $\delta_{FHDV}(k)$, which serves as a violation allowance of the bound in the soft constraint of the speed. Given the current state $x_{AV}(k+n), x_{FHDV}(k+n)$.

At the lower level, the optimal CAV control input: $U_{AV}^*(k)$ needs to fulfill the safety requirements of the LHDV. In the objective function, $r_{LHDV}(k+n) = \begin{bmatrix} l_{LHDV}^x(k+n) \\ v_{LHDV}(k+n) \end{bmatrix}$ represents the longitudinal positions and real-time velocity of the LHDV.

Lower level: CAV+LHDV

$$\min_{u_{AV},\delta_{AV}} \sum_{n=1}^{N_p} \|x_{AV}(t_{k+n}) - r_{LHDV}(t_{k+n})\|_Q^2 + \sum_{n=1}^{N_c} \|u_{AV}(t_{k+n-1})\|_R^2 + \|\delta_{AV}(t_{k+n-1})\|_P^2 \quad \textbf{(15)}$$

$s.t.(n = 1, \dots, N_p)$

$$x_{AV}(k+1) = Ax_{AV}(k) + Bu_{AV}(k) \quad \textbf{(15-1)}$$

$$x_{AV}(k+n) - r_{LHDV}(k+n) + \begin{bmatrix} l_1 \\ -\delta_{AV}(n) \end{bmatrix} \leq 0 \; for \; n = 1, \dots, N_c \quad \textbf{(15-2)}$$

$$x_{AV}(k+n) - r_{LHDV}(k+n) + \begin{bmatrix} l_1 \\ 0 \end{bmatrix} \leq 0 \; for \; n = N_p \quad \textbf{(15-3)}$$

$$d_{AV}^{max} \leq u_{AV}(k+n-1) \leq 0 \quad \textbf{(15-4)}$$

$$f(d_{FHDV}^{max}) \leq u_{AV}(k+n-1) \leq 0 \quad \textbf{(15-5)}$$

$$r_{LHDV}(k+n) - x_{AV}(k+n) + \begin{bmatrix} \sqrt{4R^2 - \left(l_{AV}^{y}(k+n) - l_{LHDV}^{y}(k+n)\right)^2} \\ -\delta_{AV}(n) \end{bmatrix} \leq 0 \quad \textbf{(15-6)}$$

$$for \; n = 1, .., N_p$$

$$\delta_{AV}(k+n) \geq 0 \quad \textbf{(15-7)}$$

With regard to the CAV's speed, the constraint can be formulated as a soft constraint to add more flexibility. $\delta_{AV}(t_i)$ denotes the violation allowance of the bound in the speed constraint. The l_{AV}^{y} in the constraint is constant, which represents the latitudinal position of CAV. $l_{LHDV}^{y}(t_i)$ represents the latitudinal position of the LHDV. The constraint of the control input of the CAV $f(d_{FHDV}^{max}, u_{FHDV})$ can be represented as:

$$f(d_{FHDV}^{max}) = \frac{2\{l_2 - P'(X_{AV}(k) - X_{FHDV}(k))\}}{\Delta t^2} + d_{FDHV}^{max} \quad \textbf{(16)}$$

$$X_{AV}(k+1) = M_x x_{AV}(k) + M_u U_{AV}(k) \quad \textbf{(16-1)}$$

$$X_{FHDV}(k+1) = M_x x_{FHDV}(k) + M_u U_{FHDV}(k) \quad \textbf{(16-2)}$$

P' represents the parameter matrix:

$$\begin{bmatrix} 1 & \Delta t & 0 & \cdots & \cdots & \cdots & 0 \\ 0 & 0 & 1 & \Delta t & 0 & \cdots & 0 \\ \vdots & \vdots & \vdots & \vdots & \vdots & \ddots & \vdots \\ 0 & 0 & 0 & 0 & 0 & 1 & \Delta t \end{bmatrix}_{N_p \times 2N_p} \quad \textbf{(16-3)}$$

For the lower-level problem, the objective function is QP, and the constraints are all linear constraints. Thus, the lower-level problem (CAV+LHDV) is a convex problem.

3.2.5 Lane-changing Maneuver MPC Controller Design and Optimization

Vehicle interaction

When the deceleration for CAV is not in the feasible range, the deceleration maneuver will be aborted in favor of the lane changing maneuver. The real time position and velocity of the PHDVs and FHDVs on the target lane will be taken into account by the MPC controller, and the lane change maneuver must be performed aggressively in order to avoid collision. the safety requirements for the FHDVs and the PHDVs are the longitudinal distances need to be satisfied and the velocity can be flexible based on the soft constraints through the lane changing process. The velocity of the FHDVs and PHDVs in the last time step need to be strictly smaller or greater than the velocity of the lane changing CAV.

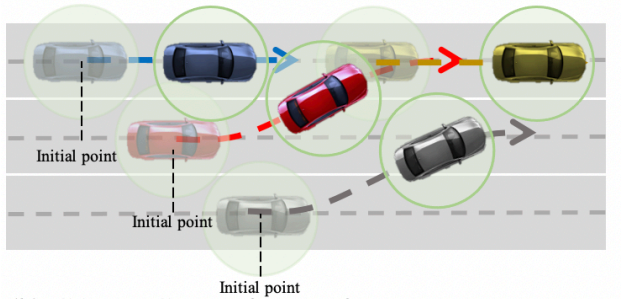

Figure 3.9. CAV and PHDVs/FHDVs interaction

As shown in Figure 3.9, the FHDV on the preceding position (FHDV-p), and the PHDV on the following position (PHDV-f) for each time step: $\left(x_{AV} - x_{FHDV-p}\right)^2 + \left(y_{FHDV-p} - y_{AV}\right)^2 = 4r^2$, $\left(x_{PHDV-f} - x_{AV}\right)^2 + \left(y_{PHDV-f} - y_{AV}\right)^2 = 4r^2$. The longitudinal distance of the FHDV is smaller than the longitudinal distance of the CAV by a constant, l_1, and the longitudinal distance of the PHDV is larger than the longitudinal of CAV by l_1 as well. During the lane change process, the velocity of the FHDV needs to be less than or equal to the velocity of the CAV, and the velocity of the PHDV needs to be larger than or equal to the velocity of the CAV. However, with soft constraints, the velocity of FHDV can exceed that of the CAV, and the velocity of PHDV

can be smaller than that of the CAV by some small values through the process. For the last time step, the velocities of the PHDV/FHDV are required to be strictly lesser/greater than or equal to the velocity of the CAV.

The interactions of FHDVs and PHDVs on the target lane are important considerations towards the bid for secondary crash avoidance as shown in Figure 3.10. The FHDV on the following position (FHDV-f) determines the feasible deceleration range for the FHDV–*p*, which is $max\{f(d^{max}_{FHDV-f}), d^{max}_{FHDV-p}\}$

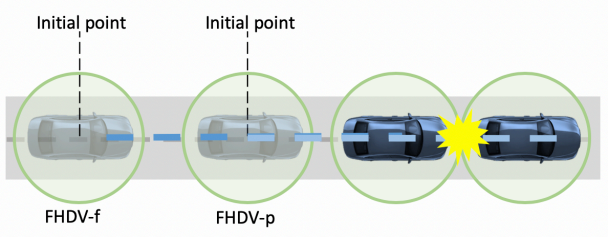

Figure 3.10. FHDVs interaction

The distance between the FHDV–*p* and the FHDV–*f* must maintain a value greater than or equal to l_2, which directly affects the headway. The maximum deceleration rate of the FHDV–*f* is d^{max}_{FHDV-f}, determined by both the comfortability and the security. The deceleration of the CAV given the FHDV is as follows:

$$f\left(d^{max}_{FHDV-f}\right) = \frac{2l_2 - 2(\Delta x + \Delta v\tau)}{\tau^2} + d^{max}_{FHDV-f} \qquad (17)$$

Where: the $\Delta x = x^i_{FHDV-p} - x^i_{FHDV-f}$, which is the initial distance between the CAV and FHDV. $\Delta v = v^i_{FHDV-p} - v^i_{FHDV-f}$.

The PHDV on the preceding position (PHDV-p) determines the feasible deceleration range for the PHDV–*f*, which is $min\{f(a^{max}_{PHDV-p}), a^{max}_{PHDV-f}\}$.

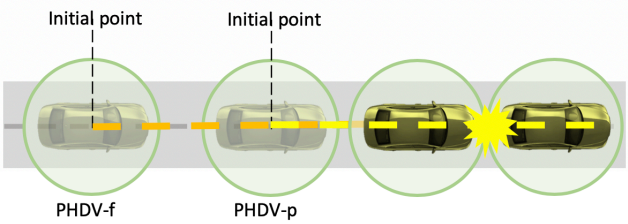

Figure 3.11. PHDVs interaction

The distance between the PHDV–*p* and the PHDV–*f* must maintain a value greater than or equal to l_2, which directly affects the headway. The maximum acceleration rate of the PHDV–*f* is a_{FHDV-f}^{max}, determined by both comfortability and security criteria. The acceleration of the PHDV-p given the PHDV-f is as follows:

$$f\left(a_{PHDV-p}^{max}\right) = \frac{-2l_2 + 2(\Delta x + \Delta v\tau)}{\tau^2} + a_{FHDV-p}^{max} \quad \textbf{(18)}$$

Where:

$\Delta x = x_{PHDV-p}^{i} - x_{PHDV-f}^{i}$, the initial distance between the CAV and FHDV.

$\Delta v = v_{PHDV-p}^{i} - v_{PHDV-f}^{i}$.

Lane-changing Maneuver Controller Design

In the lane changing maneuver, the goal is to avoid collision by diverting the CAV away from the predicted collision point. The controlled vehicles considered in this optimization problem are the PHDVs and the FHDVs in the target lane. Similar to the deceleration maneuver, the controller must satisfy the distance and velocity requirements in order to ensure safety. The FHDVs and the PHDVs are independent from each other. Therefore, in the lane changing maneuver, the control of the FHDVs and the PHDVs are two parallel bi-level MPCs. However, both need to consider the trajectory and the velocity of the CAV. Therefore, the detailed model can be formulated as follows:

With regard to the FHDVs, there are two following vehicles on the target lane that are considered in the controller: FHDV–*p*, FHDV–*f*, the detailed objective function of the FHDVs is shown as follows:

$$\min_{u_{FHDV-p},\delta_{FHDV-p},u_{FHDV-f},\delta_{FHDV-f}} F(u_{FHDV-p},\delta_{FHDV-p},u_{FHDV-f},\delta_{FHDV-f})$$

$subject\ to$:

$$u_{FHDV-p}\delta_{FHDV-p} \in \underset{u_{FHDV-p},\delta_{FHDV-p}}{\operatorname{argmin}} \left\{ \begin{matrix} f\left(u_{FHDV-p},\delta_{FHDV-p},u_{FHDV-f},\delta_{FHDV-f}\right): \\ g_j\left(u_{FHDV-p},\delta_{FHDV-p},u_{FHDV-f},\delta_{FHDV-f}\right) \le 0, j=1,\dots,J \end{matrix} \right\} \quad \textbf{(19)}$$

$$G_i\left(u_{\,FHDV-p},\delta_{FHDV-p},u_{FHDV-f},\delta_{FHDV-f}\right) \le 0, i=1,\dots,I$$

For the upper level, the cost function includes the control input variables of both the FHDVs. While at the lower level, the control input of FHDV-p needs to fulfill the safety requirements of the lane changing CAV. Thus, the detailed upper level and lower-level objective functions and constraints can be formulated as follows:

Upper level: FHDV– f + FHDV – p

$$\begin{matrix} \min\limits_{\substack{u_{FHDV-f} \\ \delta_{FHDV-f} \\ u_{FHDV-p} \\ \delta_{FHDV-p}}} & \sum_{n=1}^{N_p} \left\| x_{FHDV-f}(k+n) - x_{FHDV-p}(k+n) \right\|_Q^2 + \sum_{n=1}^{N_c} \left\| u_{FHDV-p}(k+n-1) \right\|_R^2 \\ & + \left\| u_{FHDV-f}(k+n-1) \right\|_R^2 + \left\| \delta_{FHDV-p}(k+n-1) \right\|_P^2 + \left\| \delta_{FHDV-f}(k+n-1) \right\|_P^2 \end{matrix} \quad \textbf{(20)}$$

$s.t.\ .\left(n=1,\dots,N_p\right)$

$$u_{FHDV-p},\delta_{FHDV-p} \in \underset{u_{FHDV-p},\delta_{FHDV-p}}{\operatorname{argmin}} \left\{ \begin{matrix} f(u_{AV},\delta_{AV},u_{FHDV},\delta_{FHDV}): \\ g_j(u_{AV},\delta_{AV},u_{FHDV},\delta_{FHDV}) \le 0, j=1,\dots,J \end{matrix} \right\} \quad \textbf{(20-1)}$$

$$x_{FHDV-f}(k+1) = Ax_{FHDV-f}(k) + Bu_{FHDV-f}(k) \quad \textbf{(20-2)}$$

$$x_{FHDV-f}(k+n) - x_{FHDV-p}(k+n) + \begin{bmatrix} l_2 \\ -\delta_{FHDV-f}(n) \end{bmatrix} \le 0\ for\ n=1,\dots,N_c \quad \textbf{(20-3)}$$

$$x_{FHDV-f}(k+n) - x_{FHDV-p}(k+n) + \begin{bmatrix} l_2 \\ 0 \end{bmatrix} \le 0\ for\ n=N_p \quad \textbf{(20-4)}$$

$$d_{FHDV-f}^{max} \le u_{FHDV-f}(k+n-1) \le 0 \quad \textbf{(20-5)}$$

$$\delta_{FHDV-f}(k+n) \ge 0\ n=1,\dots,N_p \quad \textbf{(20-6)}$$

The safety requirements are also considered that makes the FHDVs keep a longitudinal distance greater than l_2. $\delta_{FHDV-l}(k)$, which serves as a violation allowance of the bound in the soft constraint of the speed.

Lower level: FHDV – p + CAV

$$\min_{u_{FHDV-p},\delta_{FHDV-p}} \sum_{n=1}^{N_p} \left\| x_{FHDV-p}(t_{k+n}) - r_{LHDV}(t_{k+n}) \right\|_Q^2 + \sum_{n=1}^{N_c} \left\| u_{FHDV-p}(t_{k+n-1}) \right\|_R^2 + \left\| \delta_{FHDV-p}(t_{k+n-1}) \right\|_P^2 \quad \textbf{(21)}$$

$$s.t. (n = 1, \dots, N_p)$$

$$x_{FHDV-p}(k+1) = A x_{FHDV-p}(k) + B u_{FHDV-p}(k) \quad \textbf{(21-1)}$$

$$x_{FHDV-p}(k+n) - r_{LHDV}(k+n) + \begin{bmatrix} l_1 \\ -\delta_{FHDV-p}(n) \end{bmatrix} \leq 0 \; for \; n = 1, \dots, N_c \quad \textbf{(21-2)}$$

$$x_{FHDV-p}(k+n) - r_{LHDV}(k+n) + \begin{bmatrix} l_1 \\ 0 \end{bmatrix} \leq 0 \; for \; n = N_p \quad \textbf{(21-3)}$$

$$d_{FHDV-p}^{max} \leq u_{FHDV-p}(k+n-1) \leq 0 \quad \textbf{(21-4)}$$

$$f(d_{FHDV-f}^{max}) \leq u_{FHDV-p}(k+n-1) \leq 0 \quad \textbf{(21-5)}$$

$$r_{LHDV}(k+n) - x_{FHDV-p}(k+n) + \begin{bmatrix} \sqrt{4R^2 - \left(l_{FHDV-p}^y(k+n) - l_{LHDV}^y(k+n) \right)^2} \\ -\delta_{FHDV-p}(n) \end{bmatrix} \leq 0 \quad \textbf{(21-6)}$$

$$for \; n = 1, .., N_p$$

$$\delta_{FHDV-p}(k+n) \geq 0 \quad \textbf{(21-7)}$$

$\delta_{FHDV-p}(t_i)$ denotes the violation allowance of the bound in the speed constraint. The l_{FHDV-p}^y in the constraint is constant, which represents the latitudinal position of CAV. $l_{LHDV}^y(t_i)$ represents the latitudinal position of the LHDV. The constraint of the control input of the CAV $f(d_{FHDV-f}^{max}, u_{FHDV-p})$ is the same as the deceleration maneuvers.

With regard to the PHDVs, the focus of the objective functions is the optimal acceleration rate. The PHDVs considered here are: PHDV–*p* and PHDV–*f*. The objective function is shown as follows:

$$\min_{u_{PHDV-p},\delta_{PHDV-p},u_{PHDV-f},\delta_{PHDV-f}} F(u_{PHDV-p}, \delta_{PHDV-p}, u_{PHDV-f}, \delta_{PHDV-f}) \quad \textbf{(22)}$$

$$subject \; to:$$

$$u_{PHDV-f}, \delta_{PHDV-f} \in \underset{u_{PHDV-f}, \delta_{PHDV-f}}{\operatorname{argmin}} \begin{Bmatrix} f(u_{PHDV-p}, \delta_{PHDV-p}, u_{PHDV-f}, \delta_{PHDV-f}): \\ g_j(u_{PHDV-p}, \delta_{PHDV-p}, u_{PHDV-f}, \delta_{PHDV-f}) \leq 0, j = 1, \dots, J \end{Bmatrix}$$

$$G_i(u_{PHDV-p}, \delta_{PHDV-p}, u_{PHDV-f}, \delta_{PHDV-f}) \leq 0, i = 1, \dots, I$$

At the upper level, the cost function includes the control input variables of both the PHDVs. While at the lower level, the control input of PHDV–f needs to fulfill the safety requirements of the lane changing CAV. Thus, the detailed upper level and lower-level objective functions and constraints can be formulated as follows:

Upper level: PHDV – f + PHDV – p

$$\underset{\substack{u_{PHDV-p} \\ \delta_{PHDV-p} \\ u_{PHDV-f} \\ \delta_{PHDV-f}}}{min} \sum_{n=1}^{N_p} \left\| x_{PHDV-f}(k+n) - x_{PHDV-p}(k+n) \right\|_Q^2 + \sum_{n=1}^{N_c} \left\| u_{PHDV-p}(t_{k+n-1}) \right\|_R^2 + \left\| u_{PHDV-f}(t_{k+n-1}) \right\|_R^2 + \left\| \delta_{PHDV-p}(t_{k+n-1}) \right\|_P^2 + \left\| \delta_{PHDV-f}(t_{k+n-1}) \right\|_P^2 \quad \textbf{(23)}$$

$$s.t. (n = 1, \dots, N_p)$$

$$u_{PHDV-f}, \delta_{PHDV-f} \in \underset{u_{PHDV-f}, \delta_{PHDV-f}}{\operatorname{argmin}} \begin{Bmatrix} f(u_{PHDV-p}, \delta_{PHDV-p}, u_{PHDV-f}, \delta_{PHDV-f}): \\ g_j(u_{PHDV-p}, \delta_{PHDV-p}, u_{PHDV-f}, \delta_{PHDV-f}) \leq 0, j = 1, \dots, J \end{Bmatrix} \quad \textbf{(23-1)}$$

$$x_{PHDV-p}(k+1) = A x_{PHDV-p}(k) + B u_{PHDV-p}(k) \quad \textbf{(23-2)}$$

$$x_{PHDV-p}(k+n) - x_{PHDV-f}(k+n) - \begin{bmatrix} l_2 \\ \delta_{PHDV-p}(n) \end{bmatrix} \geq 0 \; for \; n = 1, \dots, N_c \quad \textbf{(23-3)}$$

$$x_{PHDV-p}(k+n) - x_{PHDV-f}(k+n) - \begin{bmatrix} l_2 \\ 0 \end{bmatrix} \geq 0 \; for \; n = N_p \quad \textbf{(23-4)}$$

$$0 \leq u_{PHDV-p}(k+n-1) \leq a_{PHDV-p}^{max} \quad \textbf{(23-5)}$$

$$\delta_{PHDV-p}(k+n) \leq 0 \; k = 1, \dots, N_p \quad \textbf{(23-6)}$$

The safety requirements are also considered that makes the PHDVs keep a longitudinal distance greater than l_2. Further, the speed of the PHDV–*f* of each time step needs to be no smaller than that of the PHDV–*p* by a negative value, $\delta_{PHDV-p}(k)$, which serves as a violation allowance of the bound in the soft constraint of the speed.

Lower level: PHDV– f + CAV

$$\min_{\substack{u_{PHDV-f}\\ \delta_{PHDV-f}}} \sum_{n=1}^{N_p} \left\| x_{PHDV-f}(t_{k+n}) - r_{AV}(t_{k+n}) \right\|_Q^2 + \sum_{n=1}^{N_c} \left\| u_{PHDV-f}(t_{k+n-1}) \right\|_R^2 + \left\| \delta_{PHDV-f}(t_{k+n-1}) \right\|_P^2 \quad \textbf{(24)}$$

$$s.t. (n = 1, \dots, N_p)$$

$$x_{PHDV-f}(k+1) = Ax_{PHDV-f}(k) + Bu_{PHDV-f}(k) \quad \textbf{(24-1)}$$

$$r_{AV}(k+n) - x_{PHDV-f}(k+n) + \begin{bmatrix} l_1 \\ -\delta_{PHDV-f}(n) \end{bmatrix} \leq 0 \; for \; n = 1, \dots, N_c \quad \textbf{(24-2)}$$

$$r_{AV}(k+n) - x_{PHDV-f}(k+n) + \begin{bmatrix} l_1 \\ 0 \end{bmatrix} \leq 0 \; for \; n = N_p \quad \textbf{(24-3)}$$

$$0 \leq u_{PHDV-f}(k+n-1) \leq a_{PHDV-f}^{max} \quad \textbf{(24-4)}$$

$$0 \leq u_{PHDV-f}(k+n-1) \leq f(a_{FHDV-p}^{max}) \quad \textbf{(24-5)}$$

$$r_{AV}(k+n) - x_{PHDV-f}(k+n) + \begin{bmatrix} \sqrt{4r^2 - \left(l_{PHDV-f}^{y}(k+n) - l_{AV}^{y}(k+n) \right)^2} \\ \delta_{FHDV-p}(n) \end{bmatrix} \leq 0 \quad \textbf{(24-6)}$$

$$for \; n = 1, .., N_p$$

$$\delta_{PHDV-f}(k+n) \leq 0 \quad \textbf{(24-7)}$$

At the lower level, the optimal PHDV–*f* control input: $U_{PHDV-f}^{*}(t_k)$ needs to fulfill the safety requirements of the lane changing CAV. In the objective function, $r_{AV}(t_{k+n}) = \begin{bmatrix} l_{AV}^{x}(t_{k+n}) \\ v_{AV}(t_{k+n}) \end{bmatrix}$ represents the longitudinal positions and real-time velocity of the CAV. The constraint of the control input of the CAV $f(a_{PHDV-p}^{max})$ can be represented as:

$$f(a_{PHDV-p}^{max}) = \frac{-2\left\{ l_2 - P'\left(X_{PHDV-p}(k) - X_{PHDV-f}(k) \right) \right\}}{\Delta t^2} + a_{PDHV-p}^{max} \quad \textbf{(25)}$$

$$X_{PHDV-p}(k+1) = M_x x_{PHDV-p}(k) + M_u U_{PHDV-p}(k) \quad \textbf{(25-1)}$$

$$X_{PHDV-f}(k+1) = M_x x_{PHDV-f}(k) + M_u U_{PHDV-f}(k) \quad \textbf{(25-2)}$$

Where the P' represents the same matrix mentioned in the discussion for the deceleration maneuver.

3.2.6 MPC based Controller Feasibility and Stability Analysis

Recursive feasibility analysis

One of the crucial problems in MPC is the lack of guaranteed stability and feasibility. Most of the stability proofs of MPC are based on recursive feasibility. The MPC controller is recursively feasible if and only if for all initially feasible state x_0 and for all optimal sequence of control inputs the MPC optimization problems remains feasible all the time. In order to apply the stability test, it is necessary to prove recursive feasibility. There exist sets of initial points that will ensure that the recursive feasibility of the bi-level optimal problem is satisfied. If the initial points are feasible, then the bilevel problem is recursively feasible.

Proof. Let the feasible set of the state $x_{lower}(k+n)$ represented by: S_{lower}, and the feasible set of state $x_{upper}(k+n)$ represented by: S_{upper}. Also, assume the feasible set of the control inputs $\{u_{lower}(k+n), \delta_{lower}(k+n)\}, \{u_{upper}(k+n), \delta_{upper}(k+n)\}$are C_{lower}, C_{upper}.

If $\{u_{upper}(k+n), u_{lower}(k+n), \delta_{upper}(k+n), \delta_{lower}(k+n)\}$ is feasible for the bilevel problem:$B\left(x_{lower}(k), x_{upper}(k)\right)$ with initial states $x_{lower}(k), x_{upper}(k)$, then the states $x_{lower}(k+1), x_{upper}(k+1)$ will still in the feasible sets ($x_{lower}(k+1) \in S_{lower}, x_{upper}(k+1) \in S_{upper}$) after the control inputs: $\{u_{lower}(k), \delta_{lower}(k)\}, \{u_{upper}(k), \delta_{upper}(k)\}$, which are in the feasible sets. Since the $x_{lower}(k+1) \in S_{lower}$, and the lower level: CAV-LHDV is a quadratic problem with linear constraints for$\{u_{lower}(k+1), \delta_{lower}(k+1)\}$, which is the new feasible set: C_{CAV}. The problem is convex, there will exists optimal $u_{lower}(k+1), \delta_{lower}(k+1) \in argminf(u_{lower}, \delta_{lower})$.

For the upper level, with $x_{lower}(k+1) \in S_{lower}\ and\ x_{upper}(k+1) \in S_{upper}$, optimal control inputs $u^*_{lower}(k+1), \delta^*_{lower}(k+1)$, the upper level cost function, which is also the bilevel problem objective function can be written as a quadratic programming problem as follows:

$$\begin{aligned}&\frac{1}{2}U^*_{lower}(k)^T(H_1+R)U^*_{lower}(k)+\frac{1}{2}U_{upper}(k)^T(H_2+R)U_{upper}(k)-\\&U^*_{lower}(k)^T H_3 U_{upper}(k)+x_{upper}(k)^T F_1 U_{upper}(k)-\\&x_{lower}(k)^T F_2 U_{upper}(k)+\frac{1}{2}\Delta^*_{lower}(k)^T P_1 \Delta^*_{lower}(k)+\frac{1}{2}\Delta_{upper}(k)^T P_2 \Delta_{upper}(k)\end{aligned} \quad \textbf{(26)}$$

Where: $H_1 = H_2 = H_3 = M_u^T Q M_u, F_1 = F_2 = M_u^T Q M_x$

And the Hessian matrix will be:

$$\begin{bmatrix} H_2 + R & 0 \\ 0 & P_2 \end{bmatrix}$$

Since the H_2, R, P_2 are positive. The determinants of leading principal minor of the Hessian matrix$H_2 + R$ and $(H_2 + R)P_2$ are both positive. Thus, the cost function is positive definite. Also, the constraints are all linear for $\{ u_{upper}(k+1), \delta_{upper}(k+1)\}$, which formulate a new feasible set C_{FHDV}. Then, for the upper level, with: $x_{lower}(k+1) \in S_{lower}, x_{upper}(k+1) \in S_{upper}$, and optimal control inputs of the lower level $u^*_{lower}(k+1), \delta^*_{lower}(k+1)$, there exist optimal control inputs of the upper level $u^*_{upper}(k+1), \delta^*_{upper}(k+1)$.

Thus, if there exist feasible solution for bilevel problem: $B\left(x_{lower}(k), x_{upper}(k)\right)$, then there exists feasible solution for $B\left(x_{lower}(k+1), x_{upper}(k+1)\right)$.

Sufficient condition for stability

It is well known that MPC controllers do not necessitate internal stability. Thus, it is essential to analyze and ensure the stability of the MPC controller. In order to obtain internal stability, it is common to add a final state constraint or final state penalty. However, for the MPC controller in a complex system, it is difficult to show stability using the final state constraints/final state penalty (Simon & Löfberg, 2016). All the weights are chosen to guarantee the convexity of the cost function to use the KKT condition to change the bilevel MPC to a single-level optimization problem. The sufficient condition can be proven by showing the value function is decreasing between two consecutive time steps. ($V^*_k - V^*_{k+1} \leq 0$) for any k. If the value: $V^*_k - V^*_{k+1}$ is smaller than or equal to zero for any k, which means the V_k is a valid Lyapunov function. Therefore, the system can be stabilized by the bilevel MPC controller. However, the test is only a sufficient test, not a necessary test. The system might be stable, but the Lyapunov function may not be valid for the closed loop system. However, with the sufficient stability test, there is greater chance to guarantee the stability of the system.

For both maneuvers, the Lyapunov functions are set to be the cost function of the optimization control problem, which are the higher-level objective functions of the bi-level optimization formulation. Different prediction horizon values will be tested based on the sufficient condition for stability. In this thesis, the range of the prediction horizon is $N_p = 3, \dots, 7$, the values

of the cost functions are tested to check the stability of the vehicles system after it is controlled using the bi-level MPC in deceleration/lane change maneuver.

4. NUMERICAL EXPERIMENTS AND RESULTS

This chapter presents numerical examples of the crash avoidance framework, corresponding to the two crash avoidance maneuvers discussed in earlier chapters. The experimental simulation is implemented in MATLAB using YALMIP. The simulated timestep is 0.2s. and the weights for the objective functions are specified as: $[P, Q, R] = [15,10,10]$. The safety requirements for the safety distance between the lane changing vehicles and the vehicles on the target lane is $l_1 = 5m$, the safety distance between the vehicles on the target lane is $l_2 = 10m$. The maximum deceleration as well as acceleration are assumed to be $5.08m/s^2$ (Bae et al., 2019). The maximum longitudinal acceleration is assumed to be $3.024m/s^2$ (Bokare et al., 2017). Because the interstate highway standards for the U.S. Interstate Highway System use a 12-ft. (3.7m) standard lane width (Sofield, 2018). Therefore, if the Cartesian axis origin is taken as the mid-point of the LHDV, then $l_{AV}^{y} = 3.7m$.

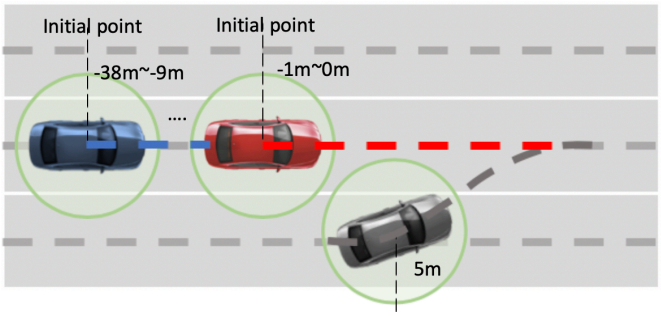

Figure 4.1. Deceleration maneuver initial states of LHDV, CAV and FHDV

In this framework, the deceleration maneuver is considered preferentially. As shown in Figure 4., the initial state of the LHDV in this example is as follows. Location: 5m, Velocity: $17.88m/s$ $(40mph)$. The initial longitudinal bumper to bumper distance between the CAV and LHDV is considered between 5m and 6m. The bumper-to-bumper distance between the CAV and FHDV is considered in the range from 5m to 34m. In order to test the performance of the control framework avoid the secondary collision (CAV and FHDV in deceleration maneuver), all the test cases have the initial velocities of the FHDV higher than the initial velocities of CAV. The velocity range of the CAV is set to be $17m/s$ to $21m/s$, the velocity range of the FHDV is set to be $18m/s$

to $22m/s$. In order to choose a proper prediction horizon to make sure the system has higher possibility to be stable, the sufficient test for stability is necessary and the results are shown in the following figure:

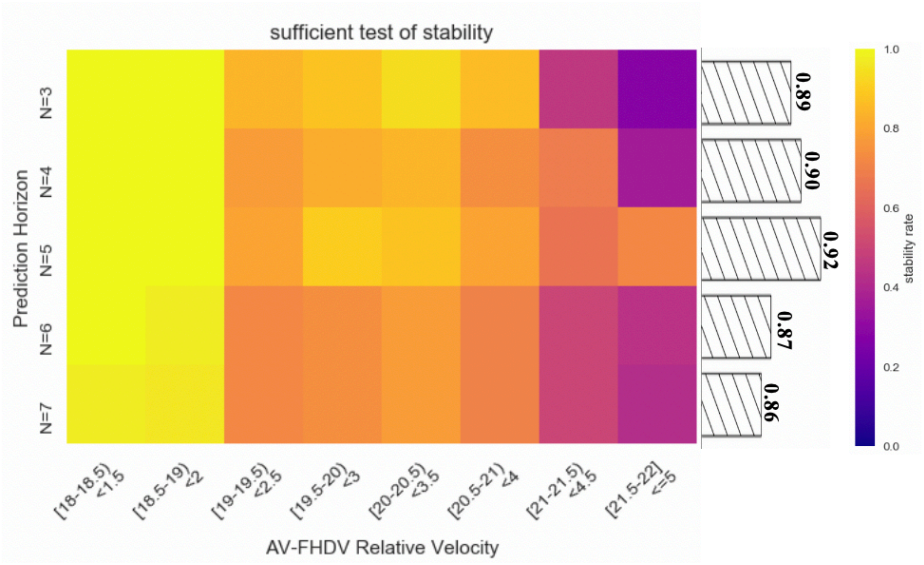

Figure 4.2. Sufficient stability test for deceleration maneuver

The range of the prediction horizon considered in this thesis is set as 7, when the controlled vehicles (CAV and FHDV) have different relative velocity, the stability rate will change. The higher the relative velocity, the lower the propensity of the system to be stable. As shown in the Figure 4.2, when N_p=5, the system has the highest probability to be sufficiently stable, which means the initial states set of the system when N_p=5 is the largest. In reality, the distribution of the velocity will also affect the choice of prediction horizon. However, in this research, we use the uniform distribution of the velocities. Thus, we choose N_p=5 in the deceleration maneuver of the MPC controller. There are some situations that deceleration might not be enough for the CAV to avoid the collision. Thus, the lane change maneuver needs to be activated. The vehicles controlled in the lane change maneuvers are the lane changing CAV, FHDVs and PHDVs on the target lane.

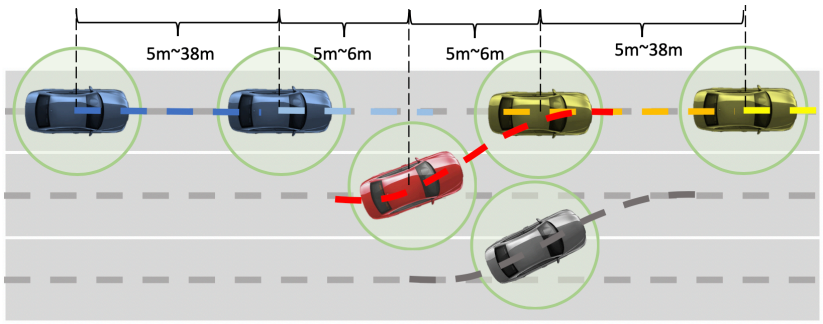

Figure 4.3. Sufficient stability test for deceleration maneuver

The initial location information of the vehicles in the lane-changing maneuver is showed in figure 4.3. The longitudinal relative distance between the CAV and vehicles on the target lane are considered between range 5m to 6m, the bumper-to-bumper distance between the FHDVs and PHDVs are considered in a wider range from 5m to 34m. The initial velocity of the vehicles on the target lane are in the range from $17m/s$ to $22m/s$, minor difference because of the positions.

The CAV velocity in the infeasible cases of the deceleration maneuver is from $17m/s$ to $21m/s$. Thus, there will be multiple lanes changing motions because of the CAV's different initial velocities in the lane changing maneuver. The sufficient stability test will be taken based on different CAV lane changing motions. The stability is various based on different CAV lane changing motions. When the speed is in the middle, around $19m/s$ to $20m/s$, the stability rates are the highest. When N_p=5, the overall stability is the highest among all the prediction horizons. Thus, we choose N_p=5 in the lane changing maneuver of the MPC controller. The successful rates of the deceleration maneuver and the deceleration + lane changing maneuvers are showed in figure 4.4(b).

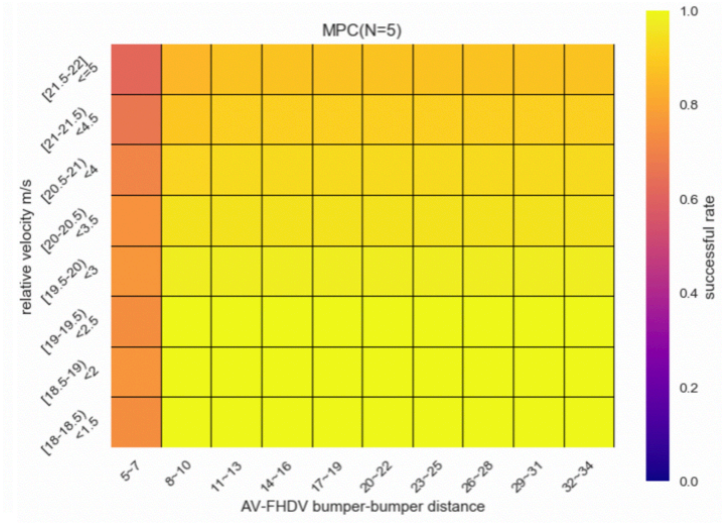

(a) Successful rates of deceleration maneuver

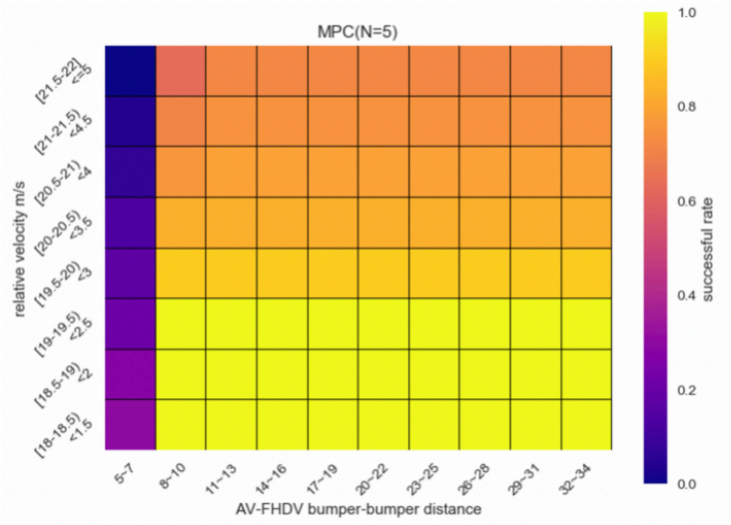

(b) Successful rates of deceleration + lane changing maneuvers

Figure 4.4. Sufficient stability test for deceleration maneuver

In figure 4.4, the successful rate is quite low (<0.4) when the bumper-to-bumper distance is smaller than 7m. Also, when the relative velocities are larger, the successful rates are not ideal. According to the lane changing maneuver, the successful rate of different CAV lane changing motions are different with different CAV lane changing motions. The overall successful rate after taking the lane changing maneuver into account is showed in figure 4.4(b). The successful rate combines the deceleration maneuver and lane changing maneuver is observed to improve significantly. The worst case, which is the largest relative velocity with smallest bumper-to-

bumper distance has successful rate more than 0.6. For the rest of situations, the successful rates are greater than 0.9, and for the cases have small relative velocity, the successful rates are 1. When the two maneuvers are taken together, the successful rates are satisfied in most cases.

Furthermore, in this thesis, we test the success rates when there is no connectivity in the system, and therefore, the traditional car-following model is used as the only means of vehicle control. The optimal velocity and optimal acceleration/decelerate rates are calculated based on the tangent condition of the circle buffer areas. The success rates are tested under different situations in terms of the bumper-to-bumper distance between the CAV and FHDV, and their relative velocities. As shown in Figure 4.5, when the bumper-to-bumper distance is smaller than 7 meters, the success rates are nearly lower than 0.2. When the relative velocities larger than 2.5m/s^2, the success rates are 0. Generally, when the bumper-to-bumper distance is larger and the relative velocities are smaller, the success rates are higher and, in some cases, reach 1.0 (i.e., 100%). Where there exists connectivity and the proposed cooperative control framework in the system, the success rates improve drastically compared to the car-following case. The overall success rates are higher when the connectivity cooperative control framework is used (average 0.9) compared to the car-following framework (average 0.4).

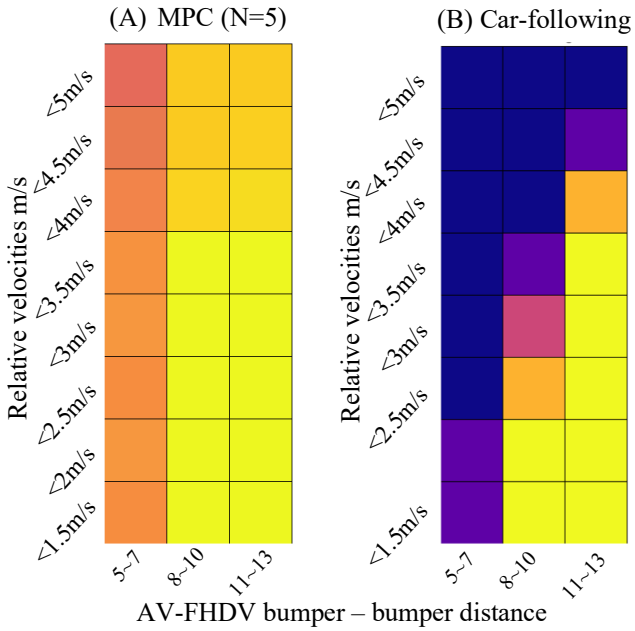

(a) Connectivity Cooperative Control Framework (b) Car-following Framework

Figure 4.5. Sufficient stability test for deceleration maneuver

5. CONCLUDING REMARKS

In order to enhance the roadway safety in the mixed traffic flow era and protect the traffic system from errant human drivers that perform lane-changing maneuvers recklessly, this paper proposes a control framework using the Model Predictive Control method based on the V2V connectivity. This framework focuses on an example of human error that cannot be eliminated by vehicle automation, specifically, human error from HDVs in the mixed traffic flow. The thesis outcomes can significantly enhance roadway safety by reducing the exposure of CAVs to errant or reckless human drivers that operate in the CAV's neighborhood. The control framework is demonstrated using numerical examples that consider various traffic setups in terms of the initial velocity as well as initial location of the controlled vehicles. The results suggest that the control framework, which contains two maneuvers (deceleration and lane-changing) has an average successful rate of collision avoidance throughout the LHDV lane-changing process of at least 90%. The successful rate can reach 100% under some specific situations such as where the relative velocity is small.

However, there exist some limitations and future work of this research. First, the velocity distribution used in this paper is uniformly distributed. In reality, the velocities of the vehicles might follow a certain pattern that may not be uniformly distributed. Second, the control framework needs to be tested in real world or a realistic driving simulator. Third, new methods including reinforcement learning can be used to provide more reliable results of the predictive aspects of the model. This thesis demonstrates the feasibility of the proposed crash avoidance framework considering vehicular interactions between the CAV and connected human-driven vehicle (CHDV), which gives a strong justification for promoting vehicle connectivity. Overall, the research outcome is expected to have far-reaching benefits in terms of public trust in AV safety, adoption of AVs, and willingness to purchase connectivity for their HDVs. On a broader front, we expect that the framework will help increase the body of knowledge and expand the understanding and awareness of techniques to enhance AV collision avoidance, and possibly influence the passage of new policies, regulation, rulemaking, or legislation associated with CAV safety and operations.

REFERENCES

[1] Anjuman, T., Hasanat-E-Rabbi, S., Siddiqui, C. K. A., & Hoque, M. M. (2020). Road traffic accident: A leading cause of the global burden of public health injuries and fatalities. In Proc Int Conf Mech Eng Dhaka Bangladesh. 200AD Dec (pp. 29-31).

[2] Babu, M., Theerthala, R. R., Singh, A. K., Baladhurgesh, B. P., Gopalakrishnan, B., Krishna, K. M., & Medasani, S. (2019, July). Model predictive control for autonomous driving considering actuator dynamics. In 2019 American Control Conference (ACC) (pp. 1983-1989). IEEE.

[3] Bae, I., Moon, J., & Seo, J. (2019). Toward a comfortable driving experience for a self-driving shuttle bus. Electronics, 8(9), 943.

[4] Bokare, P. S., & Maurya, A. K. (2017). Acceleration-deceleration behaviour of various vehicle types. Transportation research procedia, 25, 4733-4749.

[5] Camacho, E. F., & Alba, C. B. (2013). Model predictive control. Springer Science & Business Media.

[6] Chen, J., Zhao, P., Mei, T., & Liang, H. (2013, July). Lane change path planning based on piecewise bezier curve for autonomous vehicle. In Proceedings of 2013 IEEE International Conference on Vehicular Electronics and Safety (pp. 17-22). IEEE.

[7] Chen, S., Leng, Y., & Labi, S. (2020). A deep learning algorithm for simulating autonomous driving considering prior knowledge and temporal information. Computer-Aided Civil and Infrastructure Engineering, 35(4), 305-321.

[8] Chen, S., Saeed, T.U., & Labi, S. (2017). Impact of road-surface condition on rural highway safety: A multivariate random parameters negative binomial approach. Analytic Methods in Accident Research, 16, 75-89.

[9] Chen, S., Saeed, T.U., Alinizzi, M., Lavrenz, S., Labi, S. (2019). Safety sensitivity to roadway characteristics: A comparison across highway classes. Accident Analysis & Prevention, 123, 39-50.

[10] Chen, S. 2019. Safety implications of roadway design and management: new evidence and insights in the traditional and emerging (autonomous vehicle) operating environments. Ph.D. dissertation, Purdue University, West Lafayette.

[11] Chen, S., Leng, Y., Labi, S. 2020. A deep learning algorithm for simulating autonomous driving considering prior knowledge and temporal information. Computer-Aided Civil and Infrastructure Engineering, 35(4), 305-321.

[12] Christoffersen, K., & Woods, D. D. (2002). How to make automated systems team players. In Advances in human performance and cognitive engineering research (pp. 1-12). Emerald Group Publishing.

[13] Di Cairano, S., & Bemporad, A. (2009). Model predictive control tuning by controller matching. IEEE Transactions on Automatic Control, 55(1), 185-190.

[14] Dickmann, J., Appenrodt, N., Bloecher, H. L., Brenk, C., Hackbarth, T., Hahn, M., ... & Sailer, A. (2014, October). Radar contribution to highly automated driving. In 2014 44th European Microwave Conference (pp. 1715-1718). IEEE.

[15] Dong, J., Chen, S., Li, Y., Du, R., Steinfeld, A., Labi, S. 2020a. Spatio-weighted information fusion and DRL-based control for connected autonomous vehicles, IEEE ITS Conference, September 20–23, 2020. Rhodes, Greece.

[16] Dong, J., Chen, S., Li, Y., Du, R., Steinfeld, A., Labi, S. 2020b. Facilitating Connected Autonomous Vehicle Operations Using Space-weighted Information Fusion and Deep Reinforcement Learning Based Control. arXiv preprint arXiv:2009.14665.

[17] Dong, J., Chen, S., Ha, P., Du, R., Li, Y., Labi, S. 2020c. A DRL-based Multiagent Cooperative Control Framework for CAV Networks: a Graphic Convolution Q Network. arXiv preprint

[18] Du, R., Chen, S., Li, Y., Ha, P., Dong, J., Labi, S. 2020. Collision avoidance framework for autonomous vehicles under crash imminent situations. arXiv preprint

[19] Gluckman, D., 2011 Ford F-150 SuperCrew 4x2 3.7 V6 https://www.caranddriver.com/reviews/a15125561/2011-ford-f-150-37-v6-test-review/

[20] Ha, P., Chen, S., Du, R., Dong, J., Li, Y., Labi, S. 2020a. Leveraging the capabilities of connected and autonomous vehicles and multi-agent reinforcement learning to mitigate highway bottleneck congestion. arXiv preprint

[21] Ha, P., Chen, S., Du, R., Dong, J., Li, Y., Labi, S. 2020b. Vehicle connectivity and automation: A sibling relationship. Frontiers in Built Environment, 6, 199.

[22] Ji, J., Khajepour, A., Melek, W. W., & Huang, Y. (2016). Path planning and tracking for vehicle collision avoidance based on model predictive control with multiconstraints. IEEE Transactions on Vehicular Technology, 66(2), 952-964.

[23] Jia, Z., Balasuriya, A., & Challa, S. (2008). Sensor fusion-based visual target tracking for autonomous vehicles with the out-of-sequence measurements solution. Robotics and Autonomous Systems, 56(2), 157-176.

[24] Kalra, N., & Paddock, S.M. (2016). Driving to safety: How many miles of driving would it take to demonstrate autonomous vehicle reliability? Transp. Res. Part A: Policy and Practice, 94, 182-193.

[25] Kim, J., Emeršič, Ž., & Han, D. S. (2019, February). Vehicle Path Prediction based on Radar and Vision Sensor Fusion for Safe Lane Changing. In 2019 International Conference on Artificial Intelligence in Information and Communication (ICAIIC) (pp. 267-271). IEEE.

[26] Ko, M. K. (2015). U.S. Patent Application No. 14/132,249.

[27] Koopman, P., & Wagner, M. (2017). Autonomous vehicle safety: An interdisciplinary challenge. IEEE Intelligent Transportation Systems Magazine, 9(1), 90-96.

[28] Labi, S., Chen, S., Preckel, P.V., Qiao, Y., & Woldemariam, W. (2017). Rural two-lane highway shoulder and lane width policy evaluation using multiobjective optimization. Transportmetrica A: Transport Science, 13(7), 631-656.

[29] Lange, M., & Detlefsen, J. (1991). 94 GHz three-dimensional imaging radar sensor for autonomous vehicles. IEEE Transactions on Microwave Theory and Techniques, 39(5), 819-827.

[30] Lee, J. D., & Seppelt, B. D. (2006). Human factors and ergonomics in automation design. Handbook of human factors and ergonomics, 3.

[31] Li, Y., Chen, S., Dong, J., Steinfeld, A., Labi, S. 2020a. Leveraging Vehicle Connectivity and Autonomy to Stabilize Flow in Mixed Traffic Conditions: Accounting for Human-driven Vehicle Driver Behavioral Heterogeneity and Perception-reaction Time Delay. arXiv preprint arXiv:2008.04351.

[32] Li, Y., Chen, S., Du, R., Ha, P., Dong, J., Labi, S. 2020b. Using Empirical Trajectory Data to Design Connected Autonomous Vehicle Controllers for Traffic Stabilization. arXiv preprint

[33] Moosavi, S., Samavatian, M. H., Parthasarathy, S., & Ramnath, R. (2019). A Countrywide Traffic Accident Dataset. arXiv preprint arXiv:1906.05409.

[34] Naranjo, J. E., Gonzalez, C., Garcia, R., & De Pedro, T. (2008). Lane-change fuzzy control in autonomous vehicles for the overtaking maneuver. IEEE Transactions on Intelligent Transportation Systems, 9(3), 438-450.

[35] NSC (2018). Vehicle Death Estimated at 40,000 for Third Straight Year. https://www.nsc.org/road-safety/safety-topics/fatality-estimates

[36] NHTSA (2017). Vehicle-to-Vehicle Communication, National Highway Traffic Safety Administration, www.nhtsa.gov/technology-innovation/vehicle-vehicle-communication. Accessed Dec 8, 2019.

[37] Noy, I. Y., Shinar, D., & Horrey, W. J. (2018). Automated driving: Safety blind spots. Safety science, 102, 68-78.

[38] Rahman, M. S., Abdel-Aty, M., Lee, J., & Rahman, M. H. (2019). Safety benefits of arterials' crash risk under connected and automated vehicles. Transportation Research Part C: Emerging Technologies, 100, 354-371.

[39] Richter, S., Jones, C. N., & Morari, M. (2009, December). Real-time input constrained MPC using fast gradient methods. In Proceedings of the 48h IEEE Conference on Decision and Control (CDC) held jointly with 2009 28th Chinese Control Conference (pp. 7387-7393). IEEE.

[40] Richter, S., Jones, C. N., & Morari, M. (2011). Computational complexity certification for real-time MPC with input constraints based on the fast gradient method. IEEE Transactions on Automatic Control, 57(6), 1391-1403.

[41] Rivera, D. E., Morari, M., & Skogestad, S. (1986). Internal model control: PID controller design. Industrial & engineering chemistry process design and development, 25(1), 252-265.

[42] Shen, C., Guo, H., Liu, F., & Chen, H. (2017, July). MPC-based path tracking controller design for autonomous ground vehicles. In 2017 36th Chinese Control Conference (CCC) (pp. 9584-9589). IEEE.

[43] Sheridan, T.B., Parasuraman, R. (2005). Human-Automation Interaction, Reviews of Human Factors and Ergonomics 1(1):89-129, DOI: 10.1518/155723405783703082

[44] Simon, D., & Löfberg, J. (2016, December). Stability analysis of model predictive controllers using mixed integer linear programming. In 2016 IEEE 55th Conference on Decision and Control (CDC) (pp. 7270-7275). IEEE.

[45] Sinha, K.C., Labi, S. (2007). Transportation decision making: Principles of project evaluation and programming, Wiley & Sons, NY.

[46] Sofield, Tom (September 22, 2018). "Decades in the Making, I-95, Turnpike Connector Opens to Motorists". Levittown Now. Retrieved September 22, 2018.

[47] Tang, Z., Chen, S., Cheng, J., Ghahari, S. A., & Labi, S. (2018). Highway design and safety consequences: A case study of interstate highway vertical grades. Journal of Advanced Transportation, 2018. Article ID 1492614

[48] Talebpour, A., & Mahmassani, H. (2014). Modeling acceleration behavior in a connected environment. In Midyear Meetings & Symposium Celebrating 50 Years of Traffic Flow Theory (pp. 87-91).

[49] Talebpour, A., & Mahmassani, H. (2016). Influence of connected and autonomous vehicles on traffic flow stability and throughput. Transp. Research Part C: Emerging Technologies 71, 143-163.

[50] Types of vehicle accidents, Posted by Herrman & Herrman, P.L.L.C. on November 16, 2016, https://www.herrmanandherrman.com/blog/types-vehicle-accidents/

[51] United States Department of Transportation https://www.its.dot.gov/cv_basics/index.html USDOT (2011). USDOT Connected Vehicle Research Program's Vehicle-to-Vehicle Safety Application Research Plan, Tech. Report DOT HS 811 373, Washington, DC.

[52] Wang, H., Huang, Y., Khajepour, A., Zhang, Y., Rasekhipour, Y., & Cao, D. (2019). Crash mitigation in motion planning for autonomous vehicles. IEEE Transactions on Intelligent Transportation Systems, 20(9), 3313-3323.

[53] Werling, M., & Liccardo, D. (2012, December). Automatic collision avoidance using model-predictive online optimization. In 2012 IEEE 51st IEEE Conference on Decision and Control (CDC) (pp. 6309-6314). IEEE.

[54] Woo, Z. W., Chung, H. Y., & Lin, J. J. (2000). A PID type fuzzy controller with self-tuning scaling factors. Fuzzy sets and systems, 115(2), 321-326.

[55] Xu, C., Ding, Z., Wang, C., Li, Z. (2019). Statistical analysis of the patterns and characteristics of connected and autonomous vehicle involved crashes, Journal of Safety Research 71, 41-47.

[56] Yang, D., Zheng, S., Wen, C., Jin, P. J., & Ran, B. (2018). A dynamic lane-changing trajectory planning model for automated vehicles. Transportation Research Part C: Emerging Technologies, 95, 228-247.

[57] Ye, L., & Yamamoto, T. (2019). Evaluating the impact of connected and autonomous vehicles on traffic safety. Physica A: Statistical Mechanics and its Applications, 526, 121009.

[58] Zeilinger, M. N., Jones, C. N., & Morari, M. (2011). Real-time suboptimal model predictive control using a combination of explicit MPC and online optimization. IEEE Transactions on Automatic Control, 56(7), 1524-1534.